

Inelastic Flexural Stability of Corrugations

RAYMOND L. CARY

Empirically derived dimensional limits are presented for arc-and-tangent corrugated profiles to ensure local stability during inelastic bending; for example, during manufacture of culverts, storage bins, and conveyer covers. An empirical relationship for corrugation moment capacity is also presented. Twenty-four arc-and-tangent corrugated steel sheet specimens in eight corrugation and gauge combinations were tested in flexure with uniform moment. Test parameter ranges were arc inside radius-to-thickness ratios (3.7 to 27.7), tangent length-to-thickness ratios (4.4 to 23.6), and material yield strengths (40 to 50 ksi). Tangent length varied from 0.45 to 1.7 times the inside radius of the arc.

This study investigates the local stability of arc-and-tangent corrugated profiles when subjected to inelastic bending. Corrugated sheets are frequently curved to form products such as culverts, storage bins, and conveyer covers. The engineer must decide if the corrugated sheet can be satisfactorily curved without buckling. Certain structural installations may require the engineer to know the corrugation's critical flexural strain. Engineers have used experience and engineering judgment, based on elastic behavior, in developing dimensional limits for such corrugated products. Geometric limits based on elastic behavior may be unconservative, however, when corrugations sustain large inelastic strains. The engineer may also lack experience.

The only published research with some applicability to arc-and-tangent corrugated profiles deals with inelastic buckling of circular tubes. Sherman's research (1) is one example. Sherman conducted tests to determine the required outside diameter-to-thickness ratio (D/t) limit to prevent local buckling at fully developed plastic hinges. He concluded that members with D/t of 35 or less can sustain sufficient rotations to fully develop plastic hinges and failure mechanisms where $F_y = 44$ ksi. Maximum strains, however, were only about 2 percent. This is considerably less than many corrugated structures require to be successfully formed.

Sherman (1) also stated that critical strain and other inelastic buckling characteristics appears to be related to $(F_y)^{1/2}$ rather than to F_y , or to a buckling parameter of $(t/D)^2 (F_y/E)$ rather than $(t/D) (F_y/E)$.

The current study presents empirically derived relationships from 24 flexural tests that relate critical corrugation dimensional limits to critical buckling strain, minimum curving radius, and ultimate moment capacity.

EXPERIMENTAL PROGRAM

Flexural tests of corrugated profiles and material tests to determine mechanical properties were conducted. Shown in Figure 1 with key dimensions are the three commonly available corrugated profiles tested. The corrugations and material thicknesses tested are given

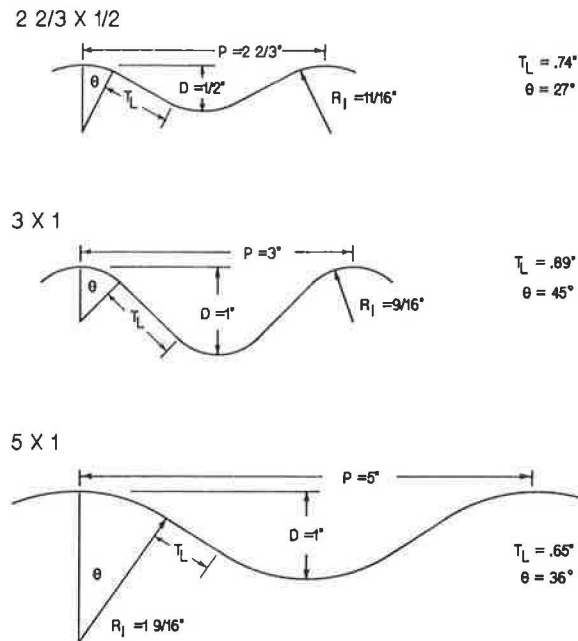


FIGURE 1 Test arc-and-tangent corrugated profiles with dimensions (T_L and θ vary slightly with gauge).

in the following table. Thickness equivalents for these U.S. standard sheet gauges are given in Table 1.

Corrugation (in.)	Thickness (gauge)
2 2/3 x 1/2	8, 14, and 20
3 x 1	8, 16, and 20
5 x 1	12 and 16

Note that 5 x 1 are nominal dimensions. This is a metric corrugation (125 x 25 mm).

Arc inside radius-to-thickness (R_i/t) ratios, tangent length-to-thickness (T_L/t) ratios, and material yield strengths (F_y) are the major parameters that affect local stability of corrugation for any given material. The selected profiles and material gauges test a broad parameter range of R_i/t (3.7 to 27.7) and T_L/t (4.4 to 23.6). Material gauges were chosen to compare corrugation behavior when either of the dimensional parameters is nearly equal in different nominal profiles.

Material Tests

Material samples were cut from a tangent portion of each corrugated sheet test specimen. Average tensile properties are given in Table 2 for the eight profile and gauge combinations. Yield strength varied from approximately 40 to 50 ksi.

TABLE 1 ABRIDGED TABLE OF THICKNESS EQUIVALENTS FOR U.S. STANDARD SHEET GAUGES

Gauge No.	U.S. Standard Gauge for Uncoated Sheet (in.)
8	0.1644
12	0.1046
14	0.0747
16	0.0598
20	0.0359

TABLE 2 MATERIAL PROPERTIES

Corrugation	Gauge	Yield Strength (ksi)	Ultimate Tensile Strength (ksi)	Elongation in 2 in. (%)
3 x 1	8	43.5	55.4	30.8
3 x 1	16	47.7	59.0	30.6
3 x 1	20	41.5	55.2	32.2
5 x 1	12	48.5	60.1	25.8
5 x 1	16	43.3	56.7	27.6
2 2/3 x 1/2	8	48.7	60.0	25.3
2 2/3 x 1/2	14	43.9	55.1	27.6
2 2/3 x 1/2	20	42.3	54.2	29.1

Note: Average of six tensile tests for each gauge.

Flexural Tests

Test Specimens

Triplicate specimens were cut for flexural testing from each corrugation profile and gauge. Each specimen was 36 in. long and three or five corrugations wide, determined by the test fixture width. Specimens were cut along the profile neutral axis to ensure that the free edge would be unstressed in flexure.

Corrugations were measured across the entire width of each specimen and dimensions averaged to calculate appropriate design properties. Key buckling parameters R_f/t and T_L/t are listed in Table 3 as average measured values for triplicate specimens.

Flexural Test Procedure

The test setup is shown in Figures 2–4. Flexural specimens are subjected to a constant moment in the 3 1/2-in.-long region

between the two center rollers. The two support rollers, 19 1/2 in. apart, and two center rollers are steel rounds machined and lubricated at each end to roll freely as the specimen deflects during the test. An 1/8-in.-thick neoprene cushion is bonded to each roller to distribute high local bearing pressures during the test over a portion of each arc. Figure 3 shows the fixture accommodating the large beam deflections necessary in this study.

A deflectionometer, shown in Figure 4, is placed in the valley of test specimen corrugations to measure specimen curvature in the center region of constant moment. The specimen's deflected shape in the constant moment region is conservatively assumed to be a circular arc. The deflectionometer consists of two pairs of legs each spanning 3 in. and a linear displacement transducer (LVDT) centered between one pair of legs. The LVDT measures deflections to the nearest 0.0001 in. in the circular arc over a fixed chord length of 3 in. between legs. With midchord deflections and chord length known, the mean arc radius of curvature can be calculated by Equation 1.

$$R_c = (4b^2 + 9)/8b - d/2 \quad (1)$$

where

$$\begin{aligned} R_c &= \text{mean radius of curvature along the corrugated profile neutral axis,} \\ b &= \text{LVDT deflection reading, and} \\ d &= \text{corrugation depth.} \end{aligned}$$

With the arc radius of curvature determined, the extreme fiber strain can be calculated by the simple flexure Equation 2.

$$\epsilon = (d + t)/2R_c \quad (2)$$

where ϵ is extreme fiber strain and t is material thickness.

Equation 2 overestimates ϵ for extreme bending to small radii of curvature. Because of neutral axis shift, the relationships in Equations 1 and 2 become complicated beyond the scope of this paper. However, any inaccuracy in the calculated strain (ϵ) is cancelled out whenever R_c is later back-calculated using strains developed from Equation 2.

Initially, strain gauges were also applied to test specimens to directly measure strains. Gauge debonding problems as well as cost discouraged the further use of strain gauges.

Loading was applied in deflection increments as recorded by the deflectionometer at midspan and held steady at each increment until the load was stable for 1 min. Usually, a 4- or 5-min maximum hold stabilized loads at each increment.

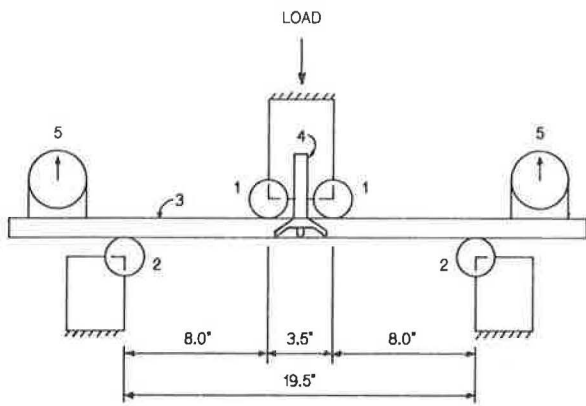
A second LVDT measured fixture vertical displacement. This

TABLE 3 MEASURED AND NORMALIZED CORRUGATION BUCKLING PARAMETERS

Corrugation	Gauge	Measured ^a		Normalized ^b	
		R_f/t	T_L/t	R_f/t_n	T_L/t_n
3 x 1	8	3.8	4.5	4.3	5.2
3 x 1	16	10.8	15.1	12.9	18.2
3 x 1	20	17.0	23.5	19.1	26.3
5 x 1	12	15.1	9.0	18.4	10.9
5 x 1	16	26.5	15.4	30.4	17.7
2 2/3 x 1/2	8	4.3	4.4	5.2	5.4
2 2/3 x 1/2	14	10.0	9.7	11.5	11.2
2 2/3 x 1/2	20	18.2	20.0	20.6	22.7

^aAverage corrugation parameters for three specimens.

^bNormalized to design $F_y = 33$ ksi by multiplying R_f/t and T_L/t ($F_y/33$)^{1/2}.



ITEM DESCRIPTION:

1. 1.75 IN. DIAMETER STEEL LOAD ROLLERS COVERED WITH .125 IN THICK NEOPRENE.
2. 1.75 IN. DIA. STEEL SUPPORT ROLLERS COVERED WITH .125 IN. THICK NEOPRENE.
3. CORRUGATED FLEXURAL TEST SPECIMEN.
4. DEFLECTOMETER TO MEASURE MIDSPAN CURVATURE.
5. MAGNETIC BASE INCLINOMETER TO MEASURE ANGULAR CHANGE OF ENDS.

FIGURE 2 Flexural test setup.

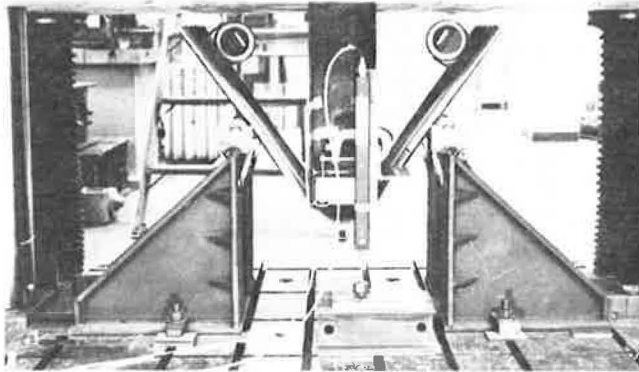


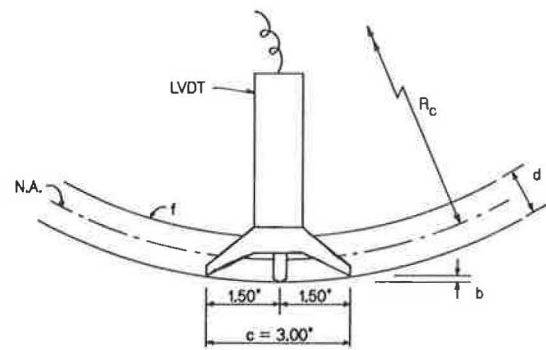
FIGURE 3 Flexural specimen during test.

displacement plus deflectometer reading, applied load, and panel rotations recorded by inclinometers enabled calculation of bending moments in the corrugated sheet. Bending moment equations are not shown because of the length and complexities caused by loads and reactions through the fixture rollers always being normal to the curved specimen. The raw data were input to a computer program that calculated bending moment, bending radius, and strain at each loading increment.

Critical Buckling Strains

The author detected initial buckling by feel, running his fingers over the multiple corrugation surfaces at each deflection increment. When surface irregularities were felt, the affected corrugation, buckled component, and deflections were recorded. Although this method is not sophisticated, it gave reasonably good replication of triplicate test results. Buckling always initiated at one of the corrugations nearest the free edge of the panel. To eliminate influence of free edges, the test specimen was not considered buckled until an interior corrugation buckled.

After testing the 3 x 1, 20-gauge specimens, it was obvious that the arcs of corrugations in compression had deformed at center



ITEM DESCRIPTION:

- b = DEFLECTOMETER DEFLECTION READING
- c = CHORD LENGTH OR DISTANCE BETWEEN DEFLECTOMETER LEGS
- d = DEPTH OF CORRUGATED SPECIMEN
- f = ASSUMED CIRCULAR ARC DEFLECTED SHAPE OF FLEXURAL SPECIMEN
- LVDT = LINEAR DISPLACEMENT TRANSDUCER
- N.A. = SPECIMEN NEUTRAL AXIS ASSUMED AT MIDDEPTH FOR ALL STRAIN LEVELS
- R_c = MEAN RADIUS OF CURVATURE

FIGURE 4 Deflectometer for measuring curvature.

load lines due to large bearing pressures from the rollers. Round bar inserts the size of the arc radius were cut 3/4 in. long. A segment equal to the corrugation height was inserted between the center rollers at each corrugation to help distribute loads more uniformly into the flexural specimen (Figure 5). The same three 20-gauge specimens were retested by cutting off the previously failed center portion and reloading. All exhibited increased strain capacity before buckling. One 3 x 1, 16-gauge specimen was retested in similar manner without a discernible difference in critical strain. Thus the other two 3 x 1, 16-gauge specimens were not retested. Thereafter all specimens tighter than 8 gauge were tested with inserts.

To account for effects from varying material yield strengths, specimen parameters R_f/t and T_L/t were normalized with respect to yield strength. As was reported by Sherman (1), less scatter was evident when data were normalized with $(F_y)^{1/2}$ instead of F_y . Thus R_f/t and T_L/t were normalized to use in design by multiplying by $(F_y/33)^{1/2}$, where F_y is the tangent tensile yield strength and 33 ksi is the AISI (2) and AASHTO (M218-82) design yield strength for buried corrugated steel structures. Normalized corrugation

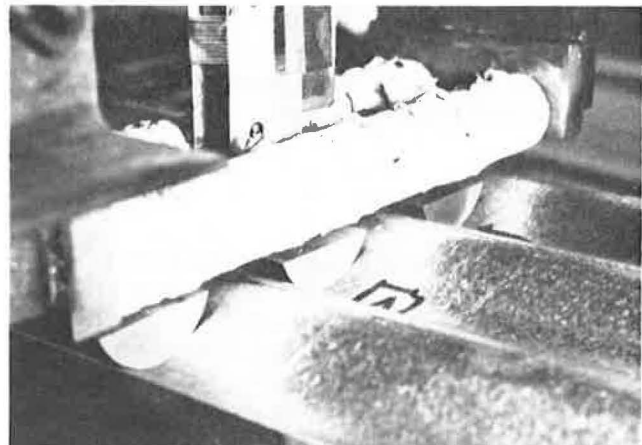


FIGURE 5 Corrugation support inserts.

parameters are shown in Table 3 along with average measured values for comparison.

Careful observation of the failure modes, critical buckling strain values, and review of numerous plots of critical strain versus normalized R_i/t and T_L/t , separately and combined, led to the conclusion that T_L/t does not significantly affect flexural buckling for the range of R_i to T_L relationships tested: $0.45 R_i \leq T_L \leq 1.7 R_i$. R_i/t is the dominant factor. If T_L is greater than R_i , buckling will be initiated in the tangents. If R_i is greater than or equal to T_L , buckling is initiated in the corrugation arcs. However, regardless of buckling mode, critical buckling strain appears to be unaffected.

Figure 6 shows a plot of nominal critical flexural strains versus normalized R_i/t (R_i/t_n). The three curves represent three possible choices for lower-bound predictions of critical strain. The first is a modified version of a lower bound for buckling of circular tubes suggested by Sherman (1). The coefficient has been modified to account for differences in design yield strengths. This curve proves

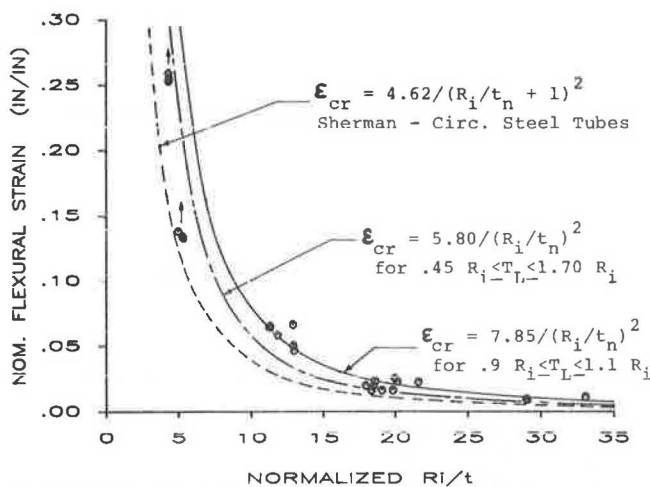


FIGURE 6 Critical flexural strain for arc-and-tangent corrugations.

to be too conservative for predicting critical strains of arc-and-tangent corrugated profiles.

The second is a general curve for the range of R_i to T_L relationships represented by the test data. Although six specimens of 8-gauge material fall below the second curve, none of the six experienced buckling. They were simply limited by the fixture geometry that would not permit additional strain to be induced. It is quite probable that corrugations with R_i/t_n of 5.5 or less will be limited by material elongation capacity rather than buckling.

The third curve appears to reasonably predict critical strains for profiles where T_L is within 10 percent of R_i values, the approximate relationship of 2 2/3 x 1/2 profile.

Ultimate Moment Capacities

T_L/t appears to be the most significant factor in determining the profile's maximum moment capacity for the range of R_i to T_L relationships tested. R_i/t factors are minor contributors. Two examples help support this conclusion. The first example compares 3 x 1, 20-gauge and 5 x 1, 12-gauge specimens. R_i/T_n factors are nearly equal, but T_L/t_n factors differ dramatically (see Table 3). The 3 x 1 T_L/t_n factors are about 26, and moment capacity averaged 94

percent of its calculated plastic moment. The 5 x 1 T_L/t_n factors are about 11, and moment capacity averaged 107 percent of its plastic moment. A second example compares the 5 x 1, 12-gauge with the 2 2/3 x 1/2, 14-gauge specimen. Here, R_i/t_n factors are different, 18.4 versus 11.5, but T_L/t_n factors for both are about 11. Both corrugations developed 107 percent of their calculated plastic moment capacity.

Figure 7 is a plot that compares maximum test moments with calculated plastic moments as a function of normalized T_L/t . Plastic moment capacity is calculated by multiplying the specimen's tangent tensile yield strength by its plastic modulus. The middle curve, labeled " M_{uc} ," is the mean of the best fit generated by a curve-fitting program. All data points are within ± 10 percent of the mean. The upper and lower curves are 95 percent confidence limits. For design, moment capacity (M_{uc}) should not exceed the plastic moment (M_p). Thus, for $T_L/t_n \leq 16$, the moment capacity equals the plastic moment.

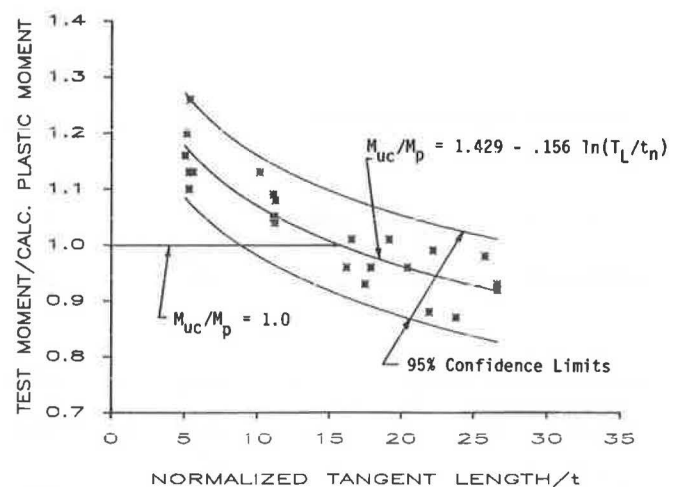


FIGURE 7 Bending moment capacity for arc-and-tangent corrugations.

DESIGN RECOMMENDATIONS

The following recommendations are based on limited test data and should not be used beyond the parameter range of $0.45 R_i \leq T_L \leq 1.7 R_i$ without further testing. Recommendations should be considered only as guidelines for corrugation design and are not intended to replace product testing.

Nominal Critical Flexural Strain

Two equations can be used for predicting nominal critical flexural strain in arc-and-tangent corrugated profiles. Equation 3 is for a specialized range of $0.9 R_i \leq T_L \leq 1.1 R_i$.

$$\epsilon_{cr} = 7.85 / (R_i/t_n)^2 \tag{3}$$

where

- ϵ_{cr} = nominal critical flexural strain,
- R_i/t_n = R_i/t normal by multiplying by $(F_y/33)^{1/2}$, and
- F_y = material yield strength in ksi.

Equation 4 is for a broader range of $0.45 R_i \leq T_L \leq 1.70 R_i$.

$$\epsilon_{cr} = 5.80/(R_i/t_n)^2 \quad (4)$$

In no case should ϵ_{cr} exceed that given in Equation 5.

$$\epsilon_{cr} \leq \text{Material elongation limit} \quad (5)$$

To achieve maximum flexural strain capacity, corrugations should be designed with R_i/t and T_L/t nearly equal and as small as possible. In addition, material should be close to the minimum yield strength of 33 ksi.

The minimum curving radius can be calculated using Equation 6 when nominal critical flexural strain is known.

$$R_c = (d + t)/2\epsilon_{cr} \quad (6)$$

where

- R_c = mean radius of curvature of the corrugated profile,
- d = corrugation depth, and
- t = material thickness.

Ultimate Moment Capacity

Arc-and-tangent corrugation ultimate moment capacity can be calculated by Equation 7.

$$M_{uc} = [1.429 - 0.156 \ln (T_L/t_n)] M_p \leq M_p \quad (7)$$

where

- M_{uc} = ultimate moment capacity,
- M_p = calculated plastic moment, and
- T_L/t_n = T_L/t normalized by multiplying by $(F_y/33)^{1/2}$.

When T_L/t_n exceeds 16 the ultimate moment capacity will be less than the calculated plastic moment (Figure 7).

SUMMARY AND CONCLUSIONS

Triplicate steel specimens in eight arc-and-tangent corrugation and gauge combinations were flexural tested to determine critical inelastic buckling strain levels and ultimate moment capacities. Specimens were 36 in. long and three or five corrugations wide. Key corrugation parameters were material yield strength (F_y), arc inside radius-to-thickness (R_i/t) and tangent length-to-thickness (T_L/t) ratios. F_y varied from 40 to 50 ksi, R_i/t from 3.7 to 27.7, and T_L/t from 4.4 to 23.6. All specimens were subjected to pure bending in the critical regions. Conclusions for arc-and-tangent corrugated steel profiles are, where $0.45 R_i \leq T_L \leq 1.7 R_i$,

1. Critical buckling strains are a function of $1/(R_i/t)^2$. T_L/t has little influence except in determining where buckling is first initiated.

2. Corrugations with R_i/t_n (normalized to 33 ksi yield strength) of 5.5 or less will probably be limited by material elongation rather than buckling.

3. Sherman's (1) equation for a lower bound of buckling in circular tubes is too conservative for corrugations.

4. Ultimate moment capacity is a function of the natural logarithm of T_L/t . T_L/t_n ratios (normalized to 33 ksi yield strength) must be 16 or less before the full plastic moment can be developed. R_i/t did not significantly affect moment capacity.

REFERENCES

1. D.R. Sherman. Tests of Circular Steel Tubes in Bending. *Journal of the Structural Division*, ASCE, Vol. 102, No. ST11, Nov. 1976, pp. 2181-2195.
2. *Handbook of Steel Drainage and Highway Construction Products*, 3rd ed. American Iron and Steel Institute, Washington, D.C., 1983.

Publication of this paper sponsored by Committee on Culverts and Hydraulic Structures.